# AZD2171: A Highly Potent, Orally Bioavailable, Vascular Endothelial Growth Factor Receptor-2 Tyrosine Kinase Inhibitor for the Treatment of Cancer

Stephen R. Wedge,[1] Jane Kendrew,[1] Laurent F. Hennequin,[4] Paula J. Valentine,[1] Simon T. Barry,[1] Sandra R. Brave,[1] Neil R. Smith,[1] Neil H. James,[1] Michael Dukes,[1] Jon O. Curwen,[1] Rosemary Chester,[1] Janet A. Jackson,[1] Sarah J. Boffey,[1] Lyndsey L. Kilburn,[1] Sharon Barnett,[1] Graham H.P. Richmond,[2] Peter F. Wadsworth,[2] Mike Walker,[3] Alison L. Bigley,[2] Sian T. Taylor,[1] Lee Cooper,[1] Sarah Beck,[1] Juliane M. Jürgensmeier,[1] and Donald J. Ogilvie[1]

[1]Cancer Bioscience, [2]Safety Assessment, and [3]Discovery DMPK, AstraZeneca, Alderley Park, Macclesfield, Cheshire, United Kingdom; and [4]AstraZeneca Pharma, Centre de Recherches, Z.I. La Pompelle, Chemin de Vrilly, Reims, France

Downloaded from http://aacrjournals.org/cancerres/article-pdf/65/10/4389/2531157/4389-4400.pdf by guest on 28 March 2025

## Abstract

**Inhibition of vascular endothelial growth factor-A (VEGF) signaling is a promising therapeutic approach that aims to stabilize the progression of solid malignancies by abrogating tumor-induced angiogenesis. This may be accomplished by inhibiting the kinase activity of VEGF receptor-2 (KDR), which has a key role in mediating VEGF-induced responses. The novel indole-ether quinazoline AZD2171 is a highly potent ($IC_{50}$ < 1 nmol/L) ATP-competitive inhibitor of recombinant KDR tyrosine kinase *in vitro*. Concordant with this activity, in human umbilical vein endothelial cells, AZD2171 inhibited VEGF-stimulated proliferation and KDR phosphorylation with $IC_{50}$ values of 0.4 and 0.5 nmol/L, respectively. In a fibroblast/endothelial cell coculture model of vessel sprouting, AZD2171 also reduced vessel area, length, and branching at subnanomolar concentrations. Once-daily oral administration of AZD2171 ablated experimental (VEGF-induced) angiogenesis *in vivo* and inhibited endochondral ossification in bone or corpora luteal development in ovary; physiologic processes that are highly dependent upon neovascularization. The growth of established human tumor xenografts (colon, lung, prostate, breast, and ovary) in athymic mice was inhibited dose-dependently by AZD2171, with chronic administration of 1.5 mg per kg per day producing statistically significant inhibition in all models. A histologic analysis of Calu-6 lung tumors treated with AZD2171 revealed a reduction in microvessel density within 52 hours that became progressively greater with the duration of treatment. These changes are indicative of vascular regression within tumors. Collectively, the data obtained with AZD2171 are consistent with potent inhibition of VEGF signaling, angiogenesis, neovascular survival, and tumor growth. AZD2171 is being developed clinically as a once-daily oral therapy for the treatment of cancer.** (Cancer Res 2005; 65(10): 4389-400)

## Introduction

Vascular endothelial growth factor-A (VEGF) is a pivotal stimulus of physiologic and pathologic angiogenesis, including the sustained neovascularization required to support solid tumor growth (1). Tumor blood vessels furnish solid malignancies with oxygen and nutrients, facilitating further dysregulated growth, and provide a route for metastatic dissemination. New vascular capillaries are derived via a complex, orchestrated series of events, involving activation of endothelial and perivascular cells and modifications to the surrounding basement membrane and extracellular matrix. Although many diverse stimuli are implicated in this process, signaling induced by VEGF is considered rate limiting. A dependency on VEGF is attributed to its ability to regulate key processes throughout the angiogenic cascade, including endothelial cell migration, proliferation and protease expression (2–4), microvascular integrin expression (5), recruitment of endothelial cell precursors (6), capillary tube formation (7), neovascular survival (8), interactions with mural cells (9), and enhanced vascular permeability (10). The production of VEGF can be disproportionately up-regulated in tumors via oncogene activation (11), loss of tumor suppressor function (12, 13), or changes in oxygen or glucose status (14). Tumor capillaries induced by overexpression of VEGF are tortuous and dilated (15); an architecture that is reminiscent of immature vessels during early vascular remodeling.

VEGF binds to the second and third immunoglobulin-like domains of its specific transmembrane receptors Flt-1 (VEGFR-1) and KDR (VEGFR-2) on endothelial cells, initiating receptor homodimerization or heterodimerization (16, 17). The conformational change induced in the receptor complex stimulates intrinsic kinase activity which transphosphorylates tyrosine residues within the cytoplasmic domains. These phosphorylated peptide sequences serve as recognition sites for Src homology 2 domain-binding proteins that subsequently propagate intracellular signaling. Activated KDR has been shown the major stimulator of angiogenesis and vascular permeability (18, 19). KDR signaling responses include (i) mitogenic signaling via activation of a phospholipase C-γ/protein kinase C/Raf/mitogen-activated protein kinase (MAPK) pathway (20), (ii) motogenic signaling through phosphorylation of FAK and paxillin (21), and (iii) survival signaling, in a complex with VE-cadherin, β-catenin, and phosphoinositide 3′-kinase (22).

With the exceptions of longitudinal bone extension during growth and cyclical changes in the female reproductive tissues, angiogenesis does not occur in healthy adults. Chronic inhibition of this process may therefore be tolerated and provide a means by which to prevent tumor progression (23). Given that KDR transduces the angiogenic effects of VEGF, and tissue expression

**Requests for reprints:** Stephen R. Wedge, Cancer and Infection Research, AstraZeneca, Mereside, Alderley Park, Macclesfield, Cheshire, SK10 4TG, United Kingdom. Phone: 44-1625-513236; Fax: 44-1625-513624; E-mail: steve.wedge@astrazeneca.com.

©2005 American Association for Cancer Research.

of this receptor is largely confined to the endothelium, inhibition of KDR signaling should provide a means for achieving selective therapeutic intervention.

A number of small molecule approaches to inhibit the intrinsic tyrosine kinase activity of KDR have been described previously, with a range of nanomolar potencies, selectivities, and pharmacokinetic properties (24–27). Here we describe AZD2171, a highly potent (subnanomolar $IC_{50}$) inhibitor of KDR tyrosine kinase and VEGF-induced signaling in endothelial cells. This compound has pharmacokinetic properties that make it suitable for chronic once-daily oral dosing. AZD2171 prevents VEGF-induced angiogenesis *in vivo* and shows dose-dependent activity in a range of human tumor xenografts in mice; statistically significant inhibition of tumor growth being evident with doses as low as 0.75 to 1.5 mg per kg per day. Furthermore, we show that inhibition of tumor growth is not merely a consequence of preventing new vessel formation; vascular regression can be observed in tumors following AZD2171 treatment.

## Materials and Methods

**AZD2171.** 4-[(4-Fluoro-2-methyl-1*H*-indol-5-yl)oxy]-6-methoxy-7-[3-(pyrrolidin-1-yl)propoxy]quinazoline (AZD2171; Fig. 1) was synthesized according to the processes described in the International Patent Application Publication Number WO 00/47212, in particular those described in Example 240 of WO/47212. The free base of AZD2171 was used in all preclinical studies, with a molecular weight of 450.51. For all *in vitro* assays, AZD2171 was prepared initially as a 10 mmol/L stock solution in DMSO and diluted in the relevant assay media. All *in vivo* studies were conducted by once-daily oral gavage. For studies in mice, AZD2171 was suspended in 1% (w/v) aqueous polysorbate 80 (polyoxyethylene; ref. 20; sorbitan mono-oleate in deionized water) and dosed at 0.1 mL/10 g of body weight. For studies in rats, AZD2171 was suspended in a 0.5% (w/v) hydroxypropyl methylcellulose solution containing 0.1% (w/v) aqueous polysorbate 80 and given at 5 mL/kg body weight.

**Kinase inhibition.** Flt-4 tyrosine kinase was obtained from ProQinase GmbH (Freiburg, Germany) and c-Kit tyrosine kinase from Upstate Biotechnology, Inc. (Lake Placid, NY). Each additional kinase used was generated as a cell lysate, following infection of insect cells with recombinant baculoviruses containing kinase domains. All enzyme assays were run at, or just below, the respective $K_m$ for ATP (0.2-30 μmol/L). The inhibitory activity of AZD2171 was determined against a range of recombinant tyrosine kinases [KDR, Flt-1, Flt-4, c-Kit, PDGFR-α, PDGFR-β, CSF-1R, Flt-3, FGFR1, Src, Abl, epidermal growth factor receptor (EGFR), ErbB2, Aur-A, and Aur-B] using ELISA methodology described previously (28). Selectivity versus CDK2 and CDK4 serine/threonine kinases was examined using scintillation proximity assays with a retinoblastoma substrate and [γ-$^{33}$P]ATP (29). Activity versus the dual specificity kinase MAPK kinase (MEK), was determined with a MAPK substrate, [γ-$^{33}$P]ATP, and paper capture/scintillation counting (29). Microcal Origin software (vs. 3.78, Microcal Software, Inc., Northhampton, MA) was used to interpolate $IC_{50}$ values by nonlinear regression.

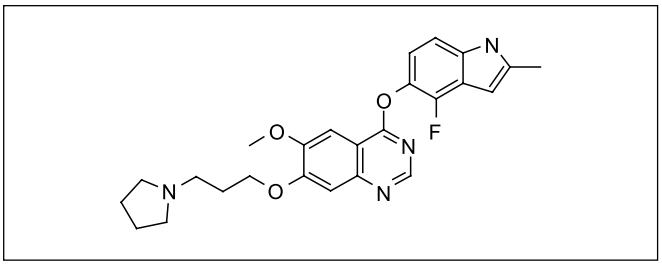


**Figure 1.** Chemical structure of AZD2171.

**Inhibition of growth factor–stimulated receptor phosphorylation.** Inhibition of receptor phosphorylation within cells was determined using ELISA (KDR and EGFR) or Western blotting (c-Kit, PDGFR-α and PDGFR-β, or Flt-3) methods, or methods incorporating a fluorescent immunocytochemical end point (CSF1-R or ErbB2). Parental cell lines were purchased from the American Type Tissue Collection (ATCC, Manassas, VA), except for MonoMac6 cells, which were obtained from the German Collection of Microorganisms and Cell Cultures (Braunschweig, Germany). With the exception of experiments examining erbB2, cells were serum starved overnight, incubated with AZD2171 for 60 to 120 minutes, and stimulated, where required, with the relevant ligand: $VEGF_{165}$ (100 ng/mL) for 7 minutes, SCF (50 ng/mL) for 10 minutes, PDGF-AA or PDGF-BB (50 ng/mL) for 5 minutes, EGF (1 μg/mL) for 3 minutes, or CSF-1 (40 ng/mL) for 10 minutes. VEGF, SCF, EGF, and CSF-1 were obtained from R&D Systems, Inc. (Abingdon, United Kingdom) and PDGF-AA and PDGF-BB from Sigma-Aldrich (Poole, United Kingdom). Inhibition of KDR phosphorylation was determined in human umbilical vein endothelial cells (HUVEC) by ELISA at ProQinase. EGFR phosphorylation was examined using a sandwich ELISA in KB human oral squamous tumor cells, with an sc-120 capture antibody (Santa Cruz Biotechnology, Inc., Santa Cruz, CA) and detection via horseradish peroxidase immunoconjugated to a 4G10 phosphotyrosine antibody (Upstate Biotechnology).

Western blotting was done using standard SDS-PAGE methods, loading 50 to 75 μg of protein per lane, with detection by enhanced chemiluminescence. Total and phosphorylated c-Kit was measured in NCI-H526 human small cell lung tumor cells, using antibodies to c-Kit (Santa Cruz Biotechnology) and phospho-c-Kit (Cell Signaling Technology, Inc., Beverly, MA). PDGFR-α and PDGFR-β phosphorylation was examined in MG63 human osteosarcoma cells, using antibodies to total (R&D Systems) and phosphorylated (Santa Cruz Biotechnology and Cell Signaling Technology) receptors. Inhibition of Flt-3 phosphorylation was investigated in MonoMac6 human acute myeloid leukemia cells, which contain an activating mutation in the juxtamembrane sequence of the receptor, using Flt-3 (Cell Signaling Technology) and phospho-Flt-3 (Cell Signaling Technology) antibodies.

ErbB2 phosphorylation was examined in MCF-7 breast carcinoma cells stably expressing constitutively activated wild-type erbB2 receptor. Cells were incubated with AZD2171 for 4 hours at 37°C, fixed in 3.3% formaldehyde/PBS, and immunostained with a phospho-erbB2 primary antibody (Santa Cruz Biotechnology) followed by an Alexa-Fluor 488 secondary antibody (Molecular Probes, Paisley, United Kingdom). ErbB2 phosphorylation was quantitated using an Acumen Explorer fluorescence laser-scanning plate reader (TTP Labtech Ltd., Royston, United Kingdom). CSF-1R phosphorylation was detected in 3T3 murine fibroblasts stably transfected with human CSF-1R. Cells were fixed in 4% formaldehyde and immunostained using a primary antibody to phosphorylated CSF-1R (Cell Signaling Technology). CSF-1R phosphorylation was quantitated using a Cellomics ArrayScan HCS Reader (Cellomics, Inc., Pittsburgh, PA).

Inhibition of KDR phosphorylation was also examined in HUVEC by Western blotting. HUVEC were serum starved overnight, incubated with AZD2171 for 90 minutes and stimulated with VEGF (50 ng/mL) for 8 minutes. Human $VEGF_{165}$ was generated as described previously (29). Antibodies against pKDR (rabbit polyclonal generated to phosphorylated Y1214), KDR (Santa Cruz Biotechnology), pMAPK (Cell Signaling Technology), or MAPK (Cell Signaling Technology) were used.

**Inhibition of growth factor–mediated cellular proliferation.** HUVEC proliferation in the presence and absence of growth factors was evaluated following a 4-day incubation by $^3$H-thymidine incorporation, as described previously (28). Proliferation of MG63 osteosarcoma cells was induced by PDGF-AA, which selectively activates PDGFR-α homodimer signaling. Cells were cultured in DMEM without phenol red (Sigma-Aldrich) containing 1% charcoal stripped FCS, 2 mmol/L glutamine, and 1% nonessential amino acids (Invitrogen, Paisley, United Kingdom) for 24 hours. AZD2171 or vehicle was added with PDGF-AA ligand (50 ng/mL; Sigma-Aldrich) and plates reincubated for 72 hours. Cellular proliferation was determined using a bromodeoxyuridine ELISA (Roche Diagnostics Ltd., Lewes, United Kingdom).

Downloaded from http://aacrjournals.org/cancerres/article-pdf/65/10/4389/2531157/4389-4400.pdf by guest on 28 March 2025

**Inhibition of tumor cell proliferation *in vitro*.** The human tumor cell lines, Calu-6 (lung carcinoma), SW620 (colorectal carcinoma), MDA-MB-231 (mammary gland adenocarcinoma), PC-3 (prostate adenocarcinoma), and SKOV-3 (ovarian adenocarcinoma) were obtained from ATCC. Cell proliferation was determined over a 3-day period as described previously (30).

**Human *in vitro* angiogenesis assay.** HUVECs and human diploid fibroblasts were obtained (day 0) as cocultures in 24-well plates (AngioKit, TCS CellWorks Ltd., Buckinghamshire, United Kingdom) and the medium immediately replaced with MCDB 131 medium (Life Technologies, Paisley, United Kingdom) containing 2% FCS, 1% glutamine, and 1% penicillin/streptomycin (Sigma, Poole, United Kingdom). AZD2171 or vehicle (0.01% DMSO in MCDB 131) was added to the cocultures. Medium, with AZD2171 or vehicle, was replenished on days 3, 6, and 8. Tubule formation was examined at day 10 following fixing and staining of tubules for CD31 (platelet/endothelial cell adhesion molecule 1) according to the manufacturer's instructions. Comparative treatment with either an antihuman VEGF neutralizing antibody or a control immunoglobulin G antibody (30 μg/mL, R&D Systems) was also examined.

To quantify tubule growth, a novel whole-well image analysis method was developed using a Zeiss KS400 3.0 Image Analyser (Imaging Associates Ltd., Bicester, United Kingdom) and a bespoke computer program. Tubule formations within each well were measured excluding a rim of 100-μm depth to avoid edge retraction artifact. The computer program segmented the images using a gray level threshold tool to select the stained cells of interest. The resultant binary images were skeletonized and nodal junctions (branch points) removed to determine the total length of an individual tubule. The branch points were counted and the total area of CD31 staining determined from the original binary image but with a correction for cells that had not migrated (labeled cells with an area of <20 μm).

**Inhibition of vascular endothelial growth factor–induced angiogenesis *in vivo*.** A Matrigel plug assay done by Vasculogen (Minneapolis, MN) was used to examine VEGF-induced angiogenesis directly. Briefly, Matrigel (0.5 mL) containing heparin (20 units/mL; Sigma Chemicals, St. Louis, MO) was diluted 3:1 in HBSS or recombinant human $VEGF_{165}$ (150 ng/mL; R&D systems) and injected s.c. into female, BALB/c athymic (*nu/nu* genotype) mice of 6 to 8 weeks of age (five per group). AZD2171 (1.5 or 6 mg per kg per day) or vehicle was given orally, from the day of Matrigel implantation, for 7 days. Matrigel plugs were recovered on day 8, one half being snap-frozen in liquid nitrogen using Tissue-Tek, ornithine carbamyl transferase compound (Fisher Scientific, Pittsburgh, PA) and the other fixed in neutral formalin and embedded in paraffin for H&E staining. Frozen sections were stained with a rat monoclonal antibody reactive to mouse CD31 conjugated to phycoerythrin (BD Biosciences PharMingen, San Diego, CA). Two sections were cut from the Matrigel samples at different levels and analyzed for vessel density. Nuclei were counterstained with 4′,6-diamidino-2-phenylindole (DAPI) and immunofluorescent images ($n$ = 7-10) of CD31 staining obtained from each sample at random. Each area was photographed under both red and UV filters. Morphometric analysis of vessel density and architecture was carried out after converting the images into a binary image using Adobe Software. Images were skeletonized using a program that converts binary data into single pixel density tracings (31). This enabled the number of vessel ends, vessel branch points (nodes), and total vessel length to be quantified with an Image Processing Toolkit (RGI, Inc., Raleigh, NC).

**Effect of AZD2171 on bone growth and luteal development.** Young female Alderley Park rats (6 weeks of age, Wistar derived, $n$ = 5) were dosed orally, once daily for 28 days with AZD2171 (1.25-5 mg per kg per day) or vehicle. Additional rats (five per group) were treated with AZD2171 (5 mg per kg per day) or vehicle for 28 days and maintained for a further 28 days without treatment, to examine the effect of compound withdrawal. Histologic paraffin wax sections of the femorotibial joints and ovaries were stained with H&E. Morphometric image analysis of femorotibial sections was done (29), with growth plate areas from both the femur and tibia in each joint being combined for an analysis of the effect of compound treatment. The area of corpora lutea in H&E-stained ovary sections was similarly determined by morphometric analysis (Joyce-Loebl Magiscan Image Analyser, Applied Imaging Ltd., Newcastle upon Tyne, United Kingdom).

***In vivo* tumor models.** Protocols for establishing s.c. PC-3, Calu-6, SKOV-3, MDA-MB-231, and SW620 tumors in female nude (*nu/nu* genotype) mice were as described previously (29, 30). When tumors reached a volume of 0.1 to 0.5 $cm^3$, mice were randomized (6-12 per group) and AZD2171 (0.75-6 mg per kg per day) or vehicle given once daily by oral gavage. Tumor volumes were assessed by bilateral Vernier caliper measurement at least twice weekly and calculated using the formula (length × width) × $\sqrt{}$ (length × width) × ($\pi$/6), where length was taken to be the longest diameter across the tumor and width the corresponding perpendicular. Growth inhibition was calculated from the start of treatment by comparison of the mean change in tumor volume for control and treated groups. To remove any size dependency before statistical evaluation (the variance in mean tumor volume data increases proportionally with volume and is therefore disproportionate between groups), data was log-transformed before statistical evaluation using a one-tailed two-sample $t$ test.

**Histologic assessment of tumor vasculature in response to AZD2171 therapy.** Mice bearing established Calu-6 human lung tumor xenografts (0.2 ± 0.01 $cm^3$, mean volume ± SE) were selected (day 0) and treated chronically with AZD2171 (6 mg per kg per day, p.o.) or vehicle. Tumors were collected (6-15 per group) 4 hours after the last dose of AZD2171 or vehicle, on days 1, 2, 7, 14, and 21. CD31 was then detected in sections using a chromagen end point or fluorescent immunostaining. CD31 staining with a chromagen end point was done on tumor specimens fixed in zinc fixative (PharMingen) using methodology described previously (29). These were analyzed blind to treatment assignment using a KS400 instrument (Imaging Associates). CD31-positive vessel number and total CD31 staining area/5,000 $\mu m^2$ viable tumor area were calculated for each section. For CD31 fluorescent immunostaining, formalin-fixed sections were incubated with a CD31 antibody (Santa Cruz Biotechnology) in serum block followed by an immunoglobulin G conjugated to Alexa Fluor 488 (Molecular Probes) and counterstained using ProLong Gold anti-fade reagent with DAPI (Molecular Probes). Fluorescent CD31 staining was visualized using an Axiovert S100 fluorescent microscope (Carl Zeiss SMT, Inc., Thornwood, NY) and images analyzed using MetaMorph version 6.1 software (Universal Imaging Co., Downingtown, PA).

## Results

**AZD2171 is a highly potent inhibitor of KDR tyrosine kinase and shows selectivity versus a range of additional kinases.** AZD2171 is a highly potent inhibitor of recombinant KDR tyrosine kinase activity *in vitro* ($IC_{50}$ < 1 nmol/L; Table 1). Additional activity is observed against the kinase associated with Flt-1 ($IC_{50}$ = 5 nmol/L) and the VEGF-C and VEGF-D receptor Flt-4 ($IC_{50} \leq 3$ nmol/L). The inhibitory activity of AZD2171 was also examined against each recombinant PDGFR-related kinase *in vitro* because of their structural similarity to the VEGF family of receptors. The $IC_{50}$ values for inhibition of c-Kit and PDGFRβ tyrosine kinase (2 and 5 nmol/L, respectively) were in a range similar to that measured versus Flt-1 and Flt-4. However, when compared with KDR kinase inhibition, AZD2171 selectivity versus the remaining PDGFR-related members ranged from >36-fold (PDGFR-α) to >1,000-fold (Flt-3). Excellent selectivity for KDR was evident versus a range of unrelated tyrosine and serine/threonine kinases, including EGFR (>1,600-fold selectivity) and MEK (>10,000-fold selectivity; Table 1). Furthermore, in addition to the data presented, no inhibition of enzyme activity was detected when 10 μmol/L of AZD2171 was examined with 100 μmol/L ATP against AMPK, ChK1, c-*jun* $NH_2$-terminal kinase, MAPK2, MSK-1, PKA, Akt/PKB, PKCα, Rock II, SAPK2b, SAPK2c, SGK, CSK, and PI 3-kinase (data not shown).

**AZD2171 inhibits vascular endothelial growth factor–induced KDR phosphorylation in human endothelial cells.** In

Downloaded from http://aacrjournals.org/cancerres/article-pdf/65/10/4389/2531157/4389-4400.pdf by guest on 28 March 2025

**Table 1.** AZD2171 inhibition of VEGF receptor tyrosine kinase activity and selectivity profile

| Kinase | $IC_{50}$ (μmol/L)*, mean ± SE |
|---|---|
| VEGFR family | |
| KDR (VEGFR-2) | <0.001 |
| Flt-1 (VEGFR-1) | 0.005 ± 0.002 |
| Flt-4 (VEGFR-3) | ≤0.003 |
| PDGFR family | |
| c-Kit | 0.002 ± 0.0001 |
| PDGFR-β | 0.005 ± 0.001 |
| PDGFR-α | 0.036 ± 0.008 |
| CSF-1R | 0.11 ± 0.03 |
| Flt-3 | >1 |
| Representatives from other kinase families | |
| FGFR1 | 0.026 ± 0.009 |
| Src | 0.13 ± 0.02 |
| Abl | 0.26 ± 0.05 |
| EGFR | 1.6 ± 0.3 |
| ErbB2 (HER-2/*neu*) | >1 |
| CDK2 | >1 |
| CDK4 | >1 |
| Aur-A | >10 |
| Aur-B | >10 |
| MEK | >10 |

*The ability of AZD2171 to inhibit human recombinant tyrosine kinase activity was examined with ATP concentrations at, or just below, the respective $K_m$. Data represent the mean ± SE of at least three separate determinations. $IC_{50}$ values quoted as "greater than" denote the inability to reach an $IC_{50}$ value with the highest concentration tested.

HUVEC, AZD2171 inhibited VEGF-stimulated phosphorylation of KDR in a dose-dependent manner with an $IC_{50}$ value of 0.0005 μmol/L (Table 2). The phosphorylation of MAPK, a downstream marker of VEGF signaling, was inhibited concomitantly (Fig. 2). To assess AZD2171 selectivity more critically, particularly between the PDGFR family of receptors, a range of cell lines were used to examine inhibition of receptor phosphorylation at a cellular level (Table 2). In comparison with inhibition of KDR phosphorylation, the AZD2171 $IC_{50}$ for inhibition of c-Kit phosphorylation in NCI-H562 cells was found only 2-fold higher, whereas 10- and 16-fold higher concentrations, respectively, were required for comparable inhibition of PDGFR-α and PDGFR-β phosphorylation in MG63 osteosarcoma cells. In accordance with the kinase selectivity profile, AZD2171 showed a high degree of selectivity (420- to >20,000-fold) for inhibition of KDR phosphorylation versus the remaining PDGFR family members, CSF-1R and Flt-3, and versus the erb family members, EGFR and erbB2 (Table 2).

**AZD2171 inhibits vascular endothelial growth factor–induced proliferation potently and shows selectivity versus mitogenesis induced by other growth factors.** Consistent with the activity shown against VEGF-stimulated KDR autophosphorylation in HUVEC, AZD2171 inhibited VEGF-stimulated HUVEC proliferation potently with an $IC_{50}$ value of 0.0004 ± 0.0002 μmol/L (Table 3). AZD2171 was found more potent against VEGF-induced HUVEC proliferation ($IC_{50}$ = 0.4 nmol/L) than other VEGFR tyrosine kinase inhibitors that have entered clinical development, including the pthalazine PTK787 ($IC_{50}$ = 0.008 ± 0.001 μmol/L, mean ± SE; $n$ = 4), the indolinone SU11248 ($IC_{50}$ = 0.04 ± 0.02 μmol/L, mean ± SD; $n$ = 2) and the isothiazole CP-547,632 ($IC_{50}$ = 0.06 ± 0.001 μmol/L, mean ± SD; $n$ = 2; data not shown). To address the functional relevance of inhibiting receptor phosphorylation in human cells, AZD2171 selectivity was examined further against proliferation induced by different growth factors. In HUVEC, AZD2171 showed selectivity of 275-fold for inhibition of VEGF-induced proliferation versus basic fibroblast growth factor (bFGF)–induced proliferation, and 1,250-fold selectivity versus an effect on EGF-induced proliferation (Table 3). The effect of AZD2171 on PDGFR-α–dependent cellular proliferation (stimulated by PDGF-AA) was examined in MG63 cells, and an $IC_{50}$ value of 0.04 μmol/L determined. This concentration is 100-fold greater than that required for comparable inhibition of VEGF-induced proliferation in HUVEC. The data indicate that AZD2171 can selectively inhibit VEGFR-dependent proliferation, in contrast to proliferation mediated by FGFR1 or EGFR, and that appreciable functional selectivity is also evident versus PDGFRα.

**Micromolar concentrations of AZD2171 are required to inhibit tumor cell proliferation directly *in vitro*.** The ability of AZD2171 to inhibit tumor cell growth directly was examined *in vitro* to ascertain whether subsequent antitumor activity *in vivo* could be ascribed to a direct antiproliferative effect or an indirect effect from inhibiting VEGF signaling. AZD2171 only inhibited tumor cell proliferation *in vitro* at comparatively high concentrations. The $IC_{50}$ values (mean ± SE) determined from three to five independent experiments against tumor cells were 3.0 ± 0.4 μmol/L (SKOV-3), 3.8 ± 0.5 μmol/L (MDA-MB-231), 5.8 ± 0.2 μmol/L (PC-3), 6.4 ± 0.6 μmol/L (Calu-6), and 7.4 ± 0.7 μmol/L (SW620). These concentrations are between 7,500- and 18,500-fold greater than required for comparable inhibition of VEGF-stimulated HUVEC proliferation and were not attained within *in vivo* tumor xenograft experiments (data not shown). The ability of AZD2171 to inhibit tumor growth *in vivo* can therefore be attributed to inhibition of VEGF signaling.

**AZD2171 inhibits tubule sprouting *in vitro* at subnanomolar concentrations and prevents VEGF-induced angiogenesis *in vivo*.** Although the complex angiogenic phenotype cannot be

**Table 2.** AZD2171 inhibition of growth factor–stimulated receptor phosphorylation

| Activated receptor | Cell line | $IC_{50}$ (μmol/L), mean ± SE | Fold selectivity versus KDR |
|---|---|---|---|
| KDR | HUVEC | 0.0005 ± 0.0003 | — |
| c-Kit | NCI-H526 | 0.001 ± 0.0003 | 2 |
| PDGFR-α | MG63 | 0.005 ± 0.0002 | 10 |
| PDGFR-β | MG63 | 0.008 ± 0.0009 | 16 |
| CSF-1R | NIH3T3/CSF1R | 0.21 ± 0.05 | 420 |
| Flt-3 | MonoMac6 | >10 | 20,000 |
| EGFR | KB | 1.1 ± 0.1 | 2,200 |
| ErbB2 | MCF-7/neu | >3 | 6,000 |

NOTE: The ability of AZD2171 to inhibit receptor phosphorylation was determined in cells following compound incubation and stimulation with the relevant ligand where required. Values represent the mean ± SE from three to four independent experiments.

Downloaded from http://aacrjournals.org/cancerres/article-pdf/65/10/4389/2531157/4389-4400.pdf by guest on 28 March 2025

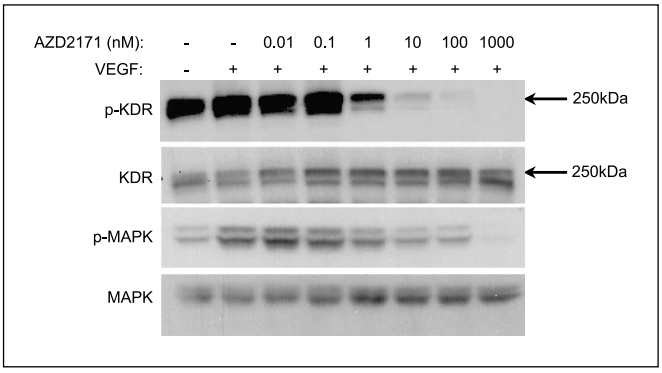


**Figure 2.** AZD2171 inhibits VEGF-stimulated KDR phosphorylation in human endothelial cells. Detection and quantitation by enhanced chemiluminescence revealed an AZD2171 $IC_{50}$ value of 0.5 nmol/L for inhibition of KDR phosphorylation that is in agreement with the value determined by ELISA (Table 2).

completely replicated *in vitro*, assays can be used to model vascular sprouting. We modified a commercially available fibroblast/endothelial cell coculture system (AngioKit, TCS CellWorks) so that exogenous bFGF was omitted from the incubation medium. Under these conditions, tubule growth is regulated more directly by VEGF, production of which increases during the course of the assay.[5] When compared with treatment with an isotype control antibody (Fig. 3*B*, *iv*) that did not affect tubule growth, a VEGF-neutralizing antibody inhibited vessel development significantly (Fig. 3*B*, *v*). Consistent with potent activity against VEGF signaling, AZD2171 inhibited vessel branching, length, and area (Fig. 3) with $IC_{50}$ values (mean ± SE; five independent experiments) of 0.0001 ± 0.00004, 0.0001 ± 0.00003, and 0.0002 ± 0.00007 μmol/L, respectively. To examine inhibition of angiogenesis *in vivo* that was selectively driven by VEGF, Matrigel plugs containing VEGF were implanted s.c. in mice and vessel development examined over the course of 8 days. AZD2171 completely abolished VEGF-induced vessel formation. The data obtained with 6 mg per kg per day AZD2171 versus number of vessel ends, branch points and total vessel length was not significantly different to that observed with 1.5 mg per kg per day (Fig. 4; $P > 0.05$ by one-tailed $t$ test). Collectively, these data show that AZD2171 is a potent inhibitor of VEGF-induced angiogenesis.

**AZD2171 induces hypertrophy in bone growth plate and inhibits luteal development in ovary: physiologic processes that are dependent upon angiogenesis.** Angiogenesis and VEGF signaling are essential events in endochondral ossification. An inhibitor of VEGF receptor tyrosine kinase activity should therefore prevent further ossification in the epiphyseal growth plates of growing animals (growth plates are closed in adults) and increase the zone of hypertrophy. AZD2171 produced a dose-dependent increase in the hypertrophic chondrocyte zone of the tibial and femoral growth plates in female rats (Fig. 5*A* and *B*). Administration of 1.25, 2.5, or 5.0 mg per kg per day AZD2171 (p.o.) increased the combined epiphyseal growth plate area by 36%, 283%, and 481%, respectively. A further 28-day period without treatment (subsequent to administration of 5 mg per kg per day AZD2171 for 28 days) resulted in complete reversal of this phenotype (Fig. 5*C*).

[5] Unpublished data.

The rapid development and growth of the ovarian corpus luteum is also critically dependent upon vascular growth. This angiogenic process is predominantly regulated by VEGF. An ovarian cycle time of only 4 days in rat means that histologic sections of an ovary reveal a dynamic picture of preovulatory and regressing follicles. Chronic administration of AZD2171 (5 mg per kg per day p.o. for 28 days) afforded a marked reduction in luteal area when compared with the ovaries of control (vehicle treated) animals (67% inhibition: Fig. 5*D* and *E*).

The effect of AZD2171 treatment on bone growth plate and ovary is supportive of inhibition of VEGF-induced angiogenesis within complex physiologic settings.

**AZD2171 shows broad-spectrum activity in human tumor models at doses that are well tolerated.** Once-daily oral administration of AZD2171 (1.5 mg per kg per day) inhibited growth of all human tumor xenografts examined in *nude* mice, irrespective of the histologic type (Table 4; Fig. 6). Statistically significant growth inhibition was obtained with 0.75 mg per kg per day AZD2171 in three of five tumor models examined, and the growth of each tumor model inhibited by >90% following administration of 6 mg per kg per day. AZD2171 treatment was well tolerated; following continuous administration of 6 mg per kg per day for 3 weeks (data accumulated from all experiments over 21 days), body weights were comparable with pretreatment values and only 1.5 % different to those of control animals (Fig. 6*B*). This is particularly notable when the weight of the additional tumor burden in control animals is considered. The broad-spectrum antitumor activity observed with AZD2171 may be attributed to a common effect on tumor vasculature, and its good tolerability to a comparatively selective profile *in vivo*.

**AZD2171 induces vascular regression in human lung tumor xenografts.** To determine whether AZD2171 affects the survival and morphology of tumor vasculature, mice bearing established Calu-6 tumors were randomized and treated chronically with AZD2171 (6 mg per kg per day) or vehicle. Mice were removed from each group at intervals to compare changes in tumor vascular area and vessel number (Fig. 7*A*). The mean control Calu-6 tumor volume was found to increase by ~6-fold over the 21-day period examined, and AZD2171 treatment was found to inhibit this tumor growth by 68% (Fig. 7*A*).

Immunohistochemical analysis of control tumors indicated that when the CD31-positive area or number of microvessels were normalized to tumor area, the values remained relatively constant throughout the duration of the experiment, irrespective

**Table 3.** AZD2171 inhibition of growth factor–stimulated cellular proliferation

| Cell type | Growth factor | $IC_{50}$ (μmol/L)*, mean ± SE | No. independent tests |
|---|---|---|---|
| HUVEC | VEGF | 0.0004 ± 0.0002 | 6 |
| | bFGF | 0.11 ± 0.01 | 9 |
| | EGF | 0.50 ± 0.09 | 9 |
| MG63 | PDGF-AA | 0.04 ± 0.007 | 3 |

*The effect of AZD2171 on growth factor–stimulated proliferation was examined using human endothelial cells (HUVEC) or MG63 human osteosarcoma tumor cells.

Downloaded from http://aacrjournals.org/cancerres/article-pdf/65/10/4389/2531157/4389-4400.pdf by guest on 28 March 2025

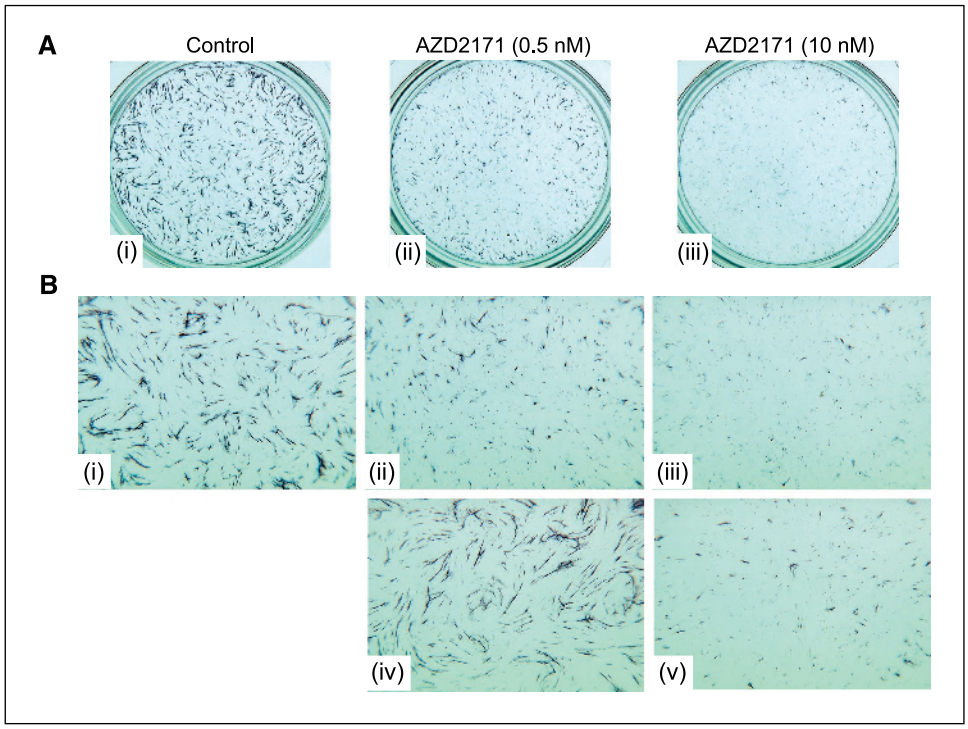


**Figure 3.** AZD2171 inhibits tubule growth *in vitro*. HUVECs and human fibroblasts were obtained as commercial cocultures (AngioKit, TCS Cellworks). Cells were maintained in MCDB 131 medium with 2% FCS in the presence or absence of AZD2171 for 10 days, after which they were fixed and immunostained for CD31. *A,* whole well (24-well plate) image of (*i*) control or AZD2171-treated cocultures [(*ii*) 0.5 nmol/L and (*iii*) 10 nmol/L]. *B,* magnification (×4) of (*i*) control, (*ii*) 0.5 nmol/L AZD2171 treated, (*iii*) 10 nmol/L AZD2171 treated, (*iv*) 30 μg/mL control immunoglobulin G antibody treated, and (*v*) following treatment with 30 μg/mL of an antihuman VEGF antibody. While the VEGF-neutralizing antibody suppressed tubule growth significantly, it remained unaffected by treatment with the isotype control. Morphometric image analysis of whole wells indicated that AZD2171 inhibited tubule branching, length, and area with an $IC_{50}$ value of ≤0.2 nmol/L.

of the accompanying volume change (Fig. 7*B* and *C*). Whereas an apparent difference ($P$ = 0.02, one-tailed $t$ test) was found between CD31 area (per 5,000 $\mu m^2$) on day 1 versus day 21, the CD31 area measured on day 1 was higher than in all subsequent groups, including day 2 where tumor volumes were directly comparable. The CD31 area on day 21 was not significantly different ($P$ = 0.3) from that measured on day 2 (Fig. 7*B*), and the vessel density (number of vessels per 5,000 $\mu m^2$) on day 21 was not significantly different from that on day 1 ($P$ = 0.3; Fig. 7*C*).

With acute AZD2171 treatment (day 1: two doses of AZD2171 given 28 and 4 hours before sampling) neither vascular variable was affected significantly. However, following an additional dose of AZD2171 (i.e., day 2: AZD2171 given at 52, 28, and 4 hours before sampling), a 47% reduction in vessel number was observed ($P$ = 0.02), accompanied by a 40% reduction in CD31 area that was just outside statistical significance ($P$ = 0.06). By day 21, vessel number and CD31 area were reduced by ≥70% ($P$ < 0.005). These data indicate that AZD2171 can cause significant vascular regression in tumors. The rapid onset of vessel regression is most probably due to a direct effect of AZD2171 on tumor endothelium, which is likely to be derived from potent inhibition of VEGF signaling.

## Discussion

Inhibition of VEGF signaling is being pursued avidly as a therapeutic strategy in oncology, to inhibit angiogenesis, neovascular survival, and vascular permeability in tumors. These VEGF-induced responses are thought dependent upon the KDR signal transduction in endothelial cells (18, 19, 32). AZD2171 may therefore have potential as an antitumor therapy, by virtue of its potent inhibitory activity against KDR tyrosine kinase. Subnanomolar $IC_{50}$ values were obtained when AZD2171 was examined against recombinant KDR kinase activity and VEGF-induced KDR phosphorylation in human endothelial cells, with concomitant inhibition of VEGF-induced phenotypes.

AZD2171 also showed activity at low nanomolar concentrations in enzyme assays, versus the kinases associated with the two other VEGF receptor family members, Flt-1 and Flt-4. The exact role of Flt-1 signaling in physiologic and pathologic angiogenesis remains unclear. Flt-1 has a relatively weak signaling capacity *in vitro* and, in contrast to KDR, a number of reports suggest that its stimulation has minimal effects on mitogenic, motogenic, or permeability responses in endothelial cells (33–35). Flt-1 with a deleted kinase domain has also been shown to support normal vascular development in mice, suggesting that Flt-1–stimulated angiogenic sprouting may be mediated by ligand sequestration, to regulate the spatial availability of VEGF, rather than via an intrinsic signaling response (36). Despite these observations, Flt-1 has been shown to co-operate directly with KDR via heterodimerization, and Flt-1 homodimers may transactivate KDR through cross-talk (37). Furthermore, Flt-1 alone can bind two additional VEGF homologues, PlGF and VEGF-B, and the former has been shown, under experimental *in vitro* conditions, to induce differential signaling through Flt-1 when compared with VEGF itself (37). These findings support the possibility that direct inhibition of Flt-1 tyrosine kinase may be beneficial. In contrast to Flt-1, Flt-4 does not bind VEGF, PlGF, or VEGF-B but only binds the homologues VEGF-C and VEGF-D. This receptor has a critical role in lymphangiogenesis (38) and a prognostic link with expression of VEGF-C and/or VEGF-D and nodal metastasis has been identified for different tumor types (39, 40). Experimentally, lymph node metastasis can be promoted by expression of VEGF-C (41) and inhibited with an antibody to Flt-4 (42). Direct inhibition of Flt-4 signaling may therefore also have therapeutic benefit in limiting subsequent tumor dissemination. However, it has recently been suggested that KDR heterodimerization (induced by VEGF-C or VEGF-D) is required for ligand-stimulated phosphorylation of Flt-4 and its

Downloaded from http://aacrjournals.org/cancerres/article-pdf/65/10/4389/2531157/4389-4400.pdf by guest on 28 March 2025

associated cellular signaling (43); a dependency that would be perturbed directly by a KDR tyrosine kinase inhibitor. Determining the full relevance of AZD2171 activity against Flt-1 and Flt-4 kinase will necessitate additional investigation of receptor signaling in cells.

The selectivity of an ATP-competitive kinase inhibitor *in vivo* is dependent upon the comparative potency of the compound against a target, the degree of inhibition required to prevent a given phenotypic effect and the level of plasma/tissue exposure attained at the evaluated dose. Collectively, the enzyme, receptor phosphorylation, and cellular proliferation data obtained with AZD2171 indicate that it has selectivity for inhibition of VEGF signaling but also suggest that it may have relevant activity versus c-Kit tyrosine kinase which could provide added therapeutic benefit in the treatment of c-Kit–dependent tumors (44, 45). That large concentrations of AZD2171 were required to inhibit the growth of tumor cells directly *in vitro*, and that AZD2171 was particularly well tolerated in tumor xenograft models at doses that proved highly efficacious, is in further support of a selective inhibitory profile.

AZD2171 combines potent activity versus KDR tyrosine kinase and selectivity with pharmacokinetic properties that are appropriate for oral once-daily administration. In female rat, studies examining i.v. (5 mg/kg) and oral (30 mg/kg) dosing of AZD2171 revealed a terminal plasma half-life of 9 hours, a relatively low clearance of 0.8 L per hour per kg, an oral bioavailability of 60%, and an unbound plasma fraction of 6% (data not shown). For this reason, all preclinical *in vivo* work was conducted by daily oral gavage.

AZD2171 treatment inhibited physiologic processes that are critically dependent upon VEGF signaling and angiogenesis. During endochondral bone formation, VEGF expression by hypertrophic chondrocytes regulates metaphyseal angiogenesis (46), with capillaries that invade the cartilage expressing both Flt-1 and KDR (47). This vascular invasion is critical to enable the terminal differentiation and apoptosis of growth plate chondrocytes, matrix resorption by osteoclasts, and mineralization by osteoblasts. The survival of osteoclasts (48) and migration and differentiation of osteoblastic cells (49, 50), both of which express Flt-1 and KDR, can also be influenced directly by VEGF signaling. Furthermore, chondrocyte survival has recently been suggested to have a VEGF dependency (51). Consistent with a fundamental regulatory role for VEGF signaling in bone morphogenesis, AZD2171 perturbed endochondral ossification in growing rats significantly and produced a marked growth plate hypertrophy; a phenotype also

Downloaded from http://aacrjournals.org/cancerres/article-pdf/65/10/4389/2531157/4389-4400.pdf by guest on 28 March 2025

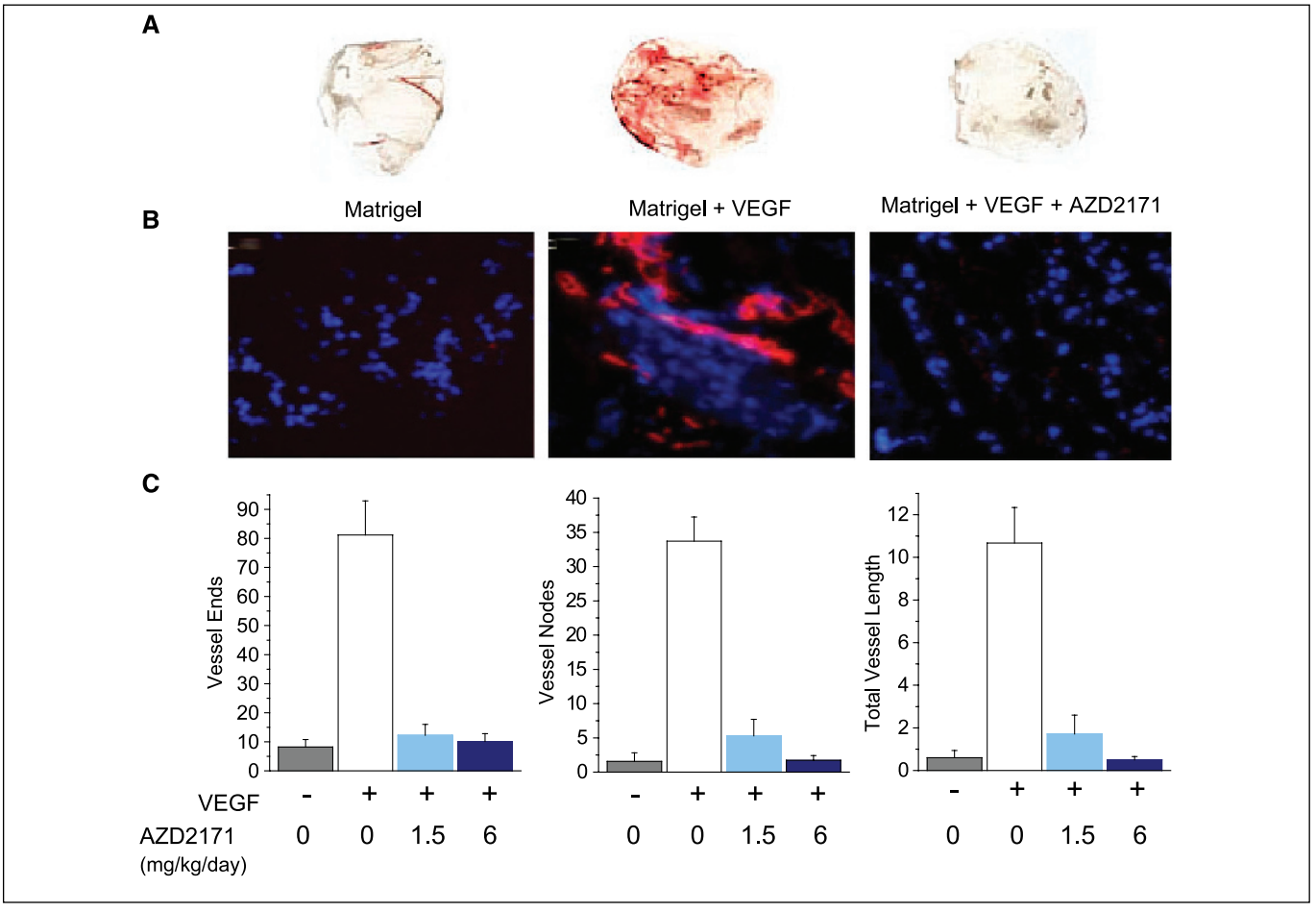


**Figure 4.** AZD2171 inhibits VEGF-induced angiogenesis *in vivo*. Matrigel plugs containing VEGF were implanted s.c. in nude mice. AZD2171 (1.5 or 6 mg per kg per day) or vehicle was administered orally, from the day of implantation, and vessel development quantitated after 8 days. *A,* representative plugs retrieved at day 8. *B,* corresponding immunofluorescent images of CD31 staining (red is anti-CD31 staining and blue is a DAPI counterstain). *C,* CD31 images from Matrigel plugs were analyzed using a skeletonization program, which enabled the number of vessel ends, branch points and total vessel length to be quantitated. Values (mean ± SE) were derived from seven to 10 independent images per sample, with five samples per group. *P*s (one-tailed *t* test) were ≤0.001 for AZD2171-treated versus control (Matrigel containing VEGF) for all variables examined.

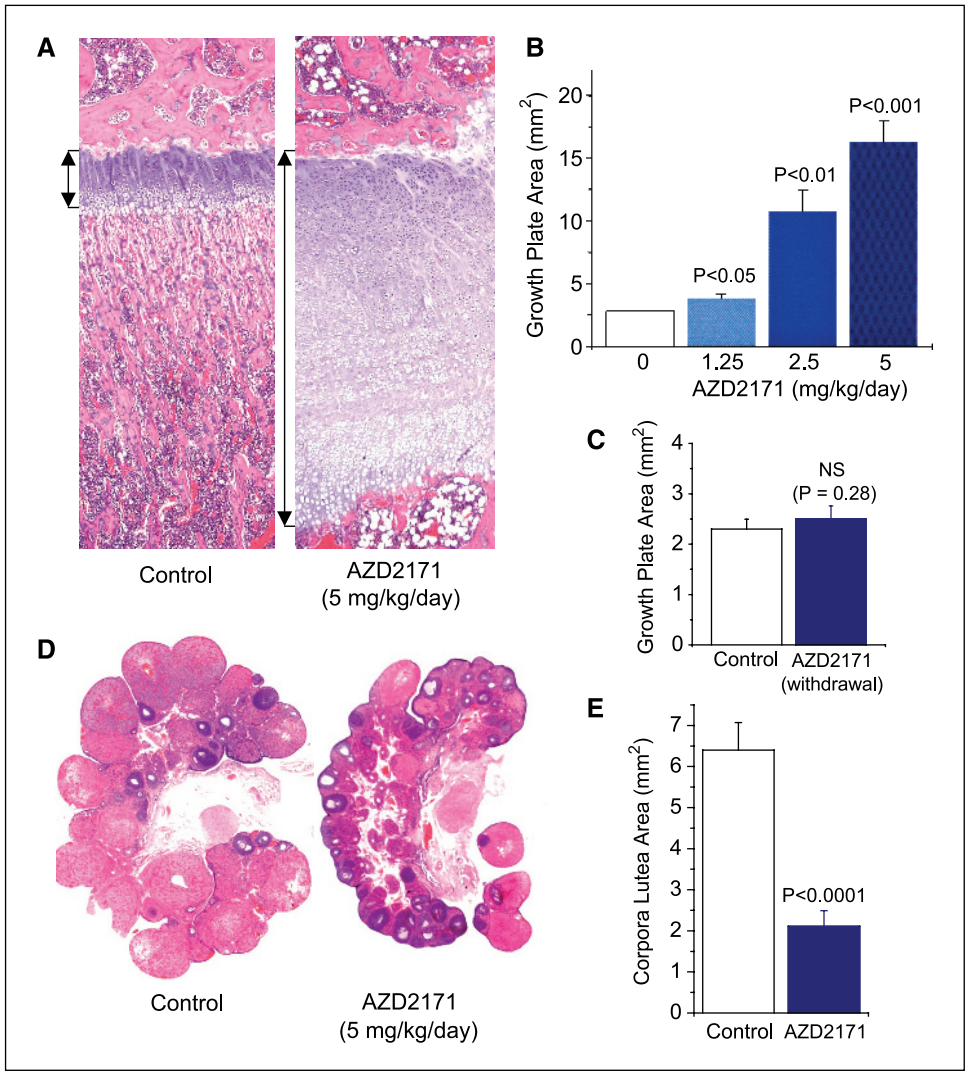


**Figure 5.** Consequences of inhibiting VEGF signaling and physiologic angiogenesis *in vivo*: effect of AZD2171 on bone morphogenesis and ovarian cycling in young female rats. *A,* H&E-stained tibial epiphyseal growth plate (×5) showing severe epiphyseal growth plate dysplasia following AZD2171 treatment (5 mg per kg per day, p.o. for 28 days). *B,* morphometric image analysis of the combined tibial and femoral growth plates following 28 days of AZD2171 treatment reveals a dose-dependent epiphyseal hypertrophy (five per group). *C,* epiphyseal hypertrophy is reversed completely 28 days after AZD2171 withdrawal (five per group). *D,* AZD2171 treatment (5 mg per kg per day, p.o. for 28 days) also induces a marked reduction in the number of corpora lutea in ovary, when compared to vehicle-treated rats. H&E-stained section, ×2.5. *E,* morphometric image analysis of total corpora lutea area (7-10 ovaries per group) following treatment with vehicle or AZD2171 (5 mg per kg per day, p.o. for 28 days). *P*s were derived using a one-tailed *t* test.

induced by VEGF sequestration (52) or conditional knockout of VEGF in cartilage (53). Whereas this phenotype has also been reported with other VEGF receptor tyrosine kinase inhibitors (26, 30), the doses of AZD2171 that produce significant effects are comparatively much lower. The magnitude of hypertrophy induced by AZD2171 has also not been shown previously. This phenotype was reversed completely following an additional 28-day period of AZD2171 withdrawal, indicating that chronic inhibition of VEGF signaling is required to maintain an effect *in vivo*. In addition to inhibiting ossification in bone growth plate, AZD2171 also markedly reduced corpora luteal area in rat ovary. The cyclic corpus luteum of the ovary is considered the site of strongest physiologic angiogenesis, with rapid luteal development involving distinct phases of VEGF-dependent blood vessel growth and maturation, followed by vessel regression during luteolysis that involves endothelial cell detachment (54). This is the first study to report the effects of a VEGF receptor kinase inhibitor on follicular development, although a soluble VEGF receptor construct has been previously found to have inhibitory effects on corpora luteal angiogenesis and development in mice (55) and a KDR blocking antibody shown to significantly delay follicular development in rhesus monkey (56). Analogous changes in bone growth plate and ovary have also been observed in primate following treatment with the VEGF-neutralizing antibody, bevacizumab (57).

AZD2171 (1.5 and 6 mg per kg per day) completely abolished VEGF-dependent angiogenesis *in vivo*, in a s.c. Matrigel plug assay, suggesting that it might also inhibit tumor growth at comparatively small doses. Doses of 6 mg per kg per day AZD2171 and lower were examined for activity in a panel of established, histologically distinct (colon, lung, prostate, breast, and ovary), human tumor xenograft models in athymic mice. Statistically significant inhibition was obtained with 1.5 mg per kg per day AZD2171 in all models and with 0.75 mg per kg per day in a number of models. The broad-spectrum antitumor profile observed with AZD2171 is consistent with an effect on tumor vasculature, a common growth-limiting target in all models, as opposed to tumor cell targets that are subject to variable expression and dependency. AZD2171 was efficacious at doses that are significantly lower than reported with other VEGFR tyrosine kinase inhibitors, which require administration within the 20 to 100 mg per kg per day range to achieve significant inhibition of tumor growth in mice (24–26).

To investigate temporal changes in tumor vessel growth and survival following AZD2171 treatment, a Calu-6 lung tumor

Downloaded from http://aacrjournals.org/cancerres/article-pdf/65/10/4389/2531157/4389-4400.pdf by guest on 28 March 2025

**Table 4.** Chronic oral once-daily administration of AZD2171 inhibits established human tumor xenograft growth

| Tumor xenograft | Tumor origin | Dose (mg/kg/d) | Tumor age at treatment onset (d) | No. doses | % Inhibition of tumor volume | Significance (*t* test, one-tailed) |
|---|---|---|---|---|---|---|
| SW620 | Colon | 6.0 | 5 | 28 | 94 | <0.001 |
| | | 3.0 | 5 | 28 | 73 | <0.001 |
| | | 1.5 | 5 | 28 | 43 | <0.001 |
| | | 0.75 | 5 | 28 | 37 | <0.01 |
| Calu-6 | Lung | 6.0 | 10 | 28 | 91 | <0.001 |
| | | 3.0 | 10 | 28 | 69 | <0.001 |
| | | 1.5 | 10 | 28 | 49 | <0.01 |
| | | 0.75 | 10 | 28 | 26 | NS |
| PC-3 | Prostate | 6.0 | 14 | 28 | 98 | <0.001 |
| | | 3.0 | 14 | 28 | 84 | <0.001 |
| | | 1.5 | 14 | 28 | 39 | <0.01 |
| | | 0.75 | 14 | 28 | 18 | NS |
| MDA-MB-231 | Breast | 6.0 | 14 | 24 | >100 | <0.001 |
| | | 3.0 | 14 | 24 | 99 | <0.001 |
| | | 1.5 | 14 | 24 | 75 | <0.001 |
| | | 0.75 | 14 | 24 | 65 | <0.001 |
| SKOV-3 | Ovary | 6.0 | 18 | 28 | >100 | <0.001 |
| | | 3.0 | 18 | 28 | >100 | <0.001 |
| | | 1.5 | 18 | 28 | 81 | <0.01 |
| | | 0.75 | 18 | 28 | 52 | <0.05 |

NOTE: Nude mice bearing established human tumor xenografts (0.1-0.5 $cm^3$ volume) were treated orally, once daily with AZD2171 (0.75-6 mg/kg/d) or vehicle [a 1% (w/v) solution of polyoxyethylene (20) sorbitan mono-oleate in deionized water]. Percentage tumor growth inhibition was calculated as the difference between the mean change in control and AZD2171-treated tumor volumes over the period of treatment. Statistical significance was examined on log-transformed data using a one-tailed *t* test (NS, $P > 0.05$). Mean control tumor volumes at the start of treatment were 0.2 $cm^3$, with the exception of SKOV-3 tumors that were 0.3 $cm^3$. Control tumor volumes at the end of vehicle treatment were 1.5 $\pm$ 0.1 $cm^3$ (SW620), 1.1 $\pm$ 0.1 $cm^3$ (Calu-6) 0.7 $\pm$ 0.1 $cm^3$ (PC-3), 1.8 $\pm$ 0.2 $cm^3$ (MDA-MB-231), and 0.9 $\pm$ 0.1 $cm^3$ (SKOV-3).
Abbreviation: NS, not significant.

xenograft model was examined, which is known to be growth inhibited by VEGF inhibition but does not regress in response to treatment (29). Vascular density in control Calu-6 tumors did not change significantly during 21 days of growth. In contrast, a comparison of vascular density in AZD2171-treated tumors with corresponding time-matched controls revealed a 47% reduction after 52 hours of treatment and a 73% reduction following 3 weeks of treatment. These data indicate that progressive vascular

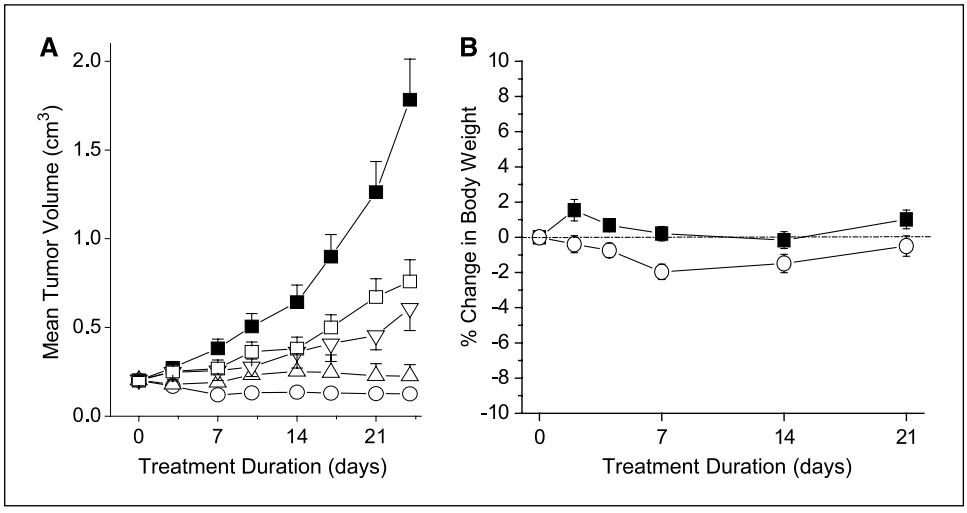


**Figure 6.** AZD2171 inhibits human tumor xenograft growth at doses that are well tolerated. *A,* effect of AZD2171 (□, 0.75 mg per kg per day; ▽, 1.5 mg per kg per day; △, 3 mg per kg per day; ○, 6 mg per kg per day) or vehicle (■) on growth of MDA-MB-231 human breast tumor xenografts. Xenografts were established s.c. in athymic mice and allowed to reach a volume of 0.2 $\pm$ 0.01 $cm^3$ (mean $\pm$ SE) before treatment. Once-daily oral administration of AZD2171 or vehicle then commenced and was continued for the duration of the experiment. *Points,* mean from 10 to 11 mice; *bars,* SE in one direction. *B,* percentage change in mouse body weight over a 21-day period, when treated chronically with vehicle (■) or 6 mg per kg per day AZD2171 (○). The analysis combines body weight data from all mice, bearing colon, lung, prostate, breast, or ovarian tumor xenografts, described in Table 4.

Downloaded from http://aacrjournals.org/cancerres/article-pdf/65/10/4389/2531157/4389-4400.pdf by guest on 28 March 2025

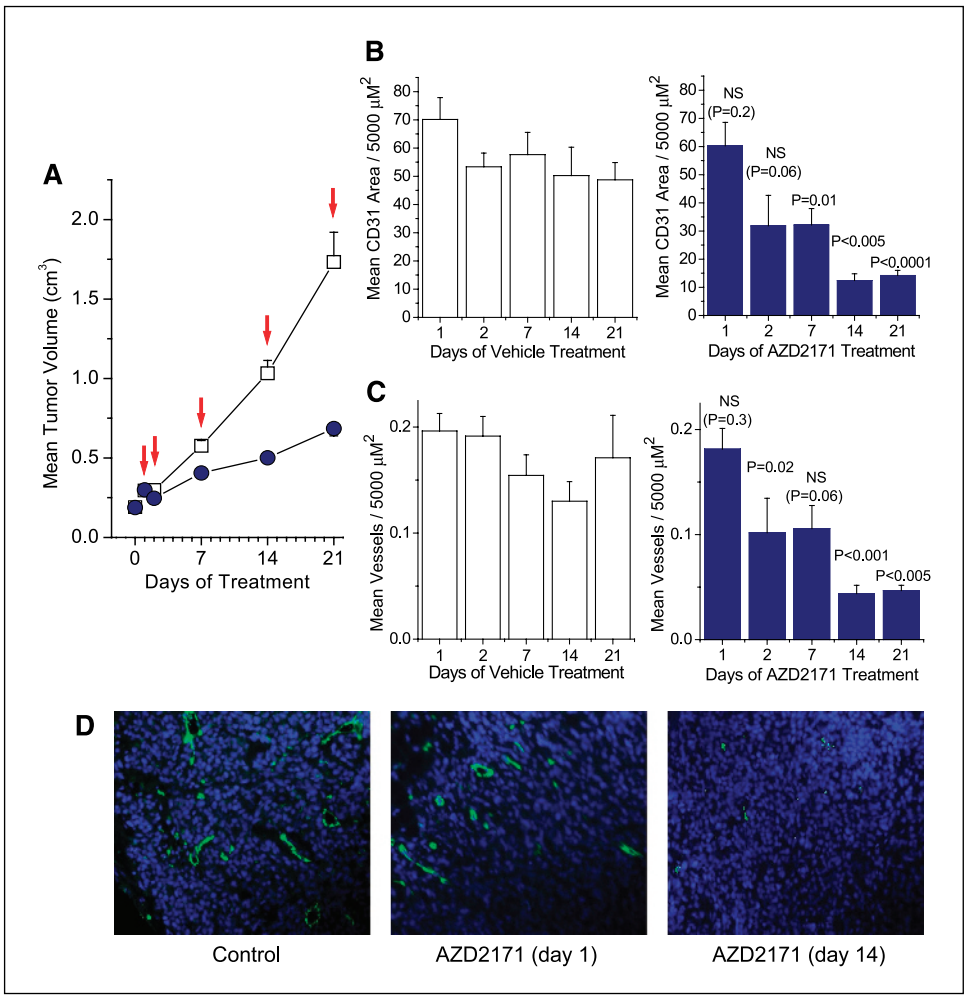


**Figure 7.** AZD2171 causes vascular regression in Calu-6 lung tumor xenografts. *A,* Calu-6 tumors were established s.c. in nude mice and treated daily (from day 0) with vehicle (□) or 6 mg per kg per day AZD2171 (●). At intervals (*arrows*) tumors ($n$ = 6-15) were collected from each group, 4 hours after dosing with vehicle or AZD2171, to enable CD31 to be determined by immunohistochemistry. *B,* mean CD31 area per 5,000 μm$^2$ of tumor and (*C*) mean vessel number per 5,000 μm$^2$ of tumor, for vehicle-treated (*open columns*) and AZD2171-treated (*blue columns*) tumors. The statistical significance of AZD2171 treatment was examined versus the respective time-matched control using a one-tailed $t$ test. While CD31 area and vessel number (both normalized to area) remain relatively constant in control tumors, a ≥70% reduction in both variables was evident following AZD2171 treatment for 21 days. *D,* immunofluorescent images of representative sections from control tumors or those treated with AZD2171 (6 mg per kg per day) and sampled on day 1 or 14. *Green,* CD31 staining; *blue,* DAPI counterstain.

regression occurs in human tumor xenografts treated chronically with AZD2171, demonstrating that inhibition of VEGF signaling can have a potent antivascular effect. A number of preclinical studies with VEGF sequestering agents have also shown evidence of reduced vascular density in tumors following treatment. These include regression of existing tumor vessels with a VEGFR-Fc fusion construct in tumor bearing RIP-Tag2 transgenic mice (58), a KDR blocking antibody in squamous cell tumor xenografts (59), and a VEGF-neutralizing antibody in LS174T colon tumor xenografts (60). Primitive vessels are believed to be susceptible to VEGF blockade, because their survival is highly dependent upon KDR mediated Akt/PKB signaling (8). These data serve to emphasize that the consequences of inhibiting VEGF signaling in pathologic conditions may extend beyond simply preventing new vessel growth.

That inhibition of VEGF signaling can provide clinical benefit to patients with solid tumors, has been confirmed recently by bevacizumab (Avastin, Genentech, South San Francisco, CA), a monoclonal antibody to VEGF-A. In combination with irinotecan, 5-fluorouracil and leucovorin, bevacizumab imparts a significant prolongation of survival and response variables in patients with first-line metastatic colorectal cancer (61). An additional small preoperative biomarker study has also suggested antivascular effects in rectal carcinoma patients, following bevacizumab treatment (62). Direct inhibition of KDR tyrosine kinase activity with a small molecule, such as AZD2171, is an alternative therapeutic approach that may afford advantages to sequestration of VEGF. Inhibiting the kinase domain of KDR is mechanistically different, in that it should prevent receptor signaling irrespective of the activating ligand. In addition to VEGF-A, the fully proteolytically cleaved forms of the related VEGF gene family members VEGF-C and VEGF-D can also bind to and activate KDR (63, 64). In particular, VEGF-C can induce proliferative, migratory, tubulogenic, and permeability responses through KDR (63, 65). Chronic administration of a small molecule to generate steady state plasma levels may also provide a pharmacokinetic advantage, because the distribution and clearance of a large biopharmaceutical may possibly be influenced more highly by heterogeneous tumor anatomy and variable tumor blood flow (66).

In summary, AZD2171 is a highly potent inhibitor of KDR tyrosine kinase that has pharmacokinetic properties suitable for once-daily oral administration. VEGF-induced angiogenesis, neovascular survival, and growth of human tumor xenografts, are inhibited significantly by AZD2171, at comparatively low doses. AZD2171 is currently being evaluated in clinical trials as a once-daily oral therapy for the treatment of a variety of malignancies. Encouragingly, these clinical studies indicate that AZD2171 retains a good pharmacokinetic profile in man, with dose-proportional increases in plasma exposure and a mean terminal plasma half-life of 20 hours (67).

Downloaded from http://aacrjournals.org/cancerres/article-pdf/65/10/4389/2531157/4389-4400.pdf by guest on 28 March 2025

## Acknowledgments

Received 12/9/2004; revised 2/16/2005; accepted 3/2/2005.

The costs of publication of this article were defrayed in part by the payment of page charges. This article must therefore be hereby marked *advertisement* in accordance with 18 U.S.C. Section 1734 solely to indicate this fact.

We thank Karen Malbon, Claire Barnes, Minwei Ye, Stephen Brightwell, John Stawpert, and Sandra Oakes for the technical assistance in selectivity testing; Kevin Randal for morphometric image analysis; David Blowers, Ian Taylor, Hazel Weir, and Rick Davies for protein production and purification; Mick Shaw for the isolation and supply of HUVECs; and Michel Vautier for doing the initial synthesis of AZD2171.

## References

1. Ferrara N. VEGF and the quest for tumour angiogenesis factors. Nat Rev Cancer 2002;2:795–803.
2. Rousseau S, Houle F, Huot J. Integrating the VEGF signals leading to actin-based motility in vascular endothelial cells. Trends Cardiovasc Med 2000;10:321–7.
3. Keck PJ, Hauser SD, Krivi G, et al. Vascular permeability factor, an endothelial cell mitogen related to PDGF. Science (Washington DC) 1989;246:1309–12.
4. Lamoreaux WJ, Fitzgerald ME, Reiner A, Hasty KA, Charles ST. Vascular endothelial growth factor increases release of gelatinase A and decreases release of tissue inhibitor of metalloproteinases by microvascular endothelial cells *in vitro*. Microvasc Res 1998;55:29–42.
5. Senger DR, Ledbetter SR, Claffey KP, Papadopoulos-Sergio A, Perruzzi CA, Detmar M. Stimulation of endothelial cell migration by vascular endothelial growth factor through cooperative mechanisms involving the αvβ3 integrin, osteopontin, and thrombin. Am J Pathol 1996;149:293–305.
6. Asahara T, Takahashi T, Masuda H, et al. VEGF contributes to postnatal neovascularisation by mobilizing bone marrow-derived endothelial progenitor cells. EMBO J 1999;18:3964–72.
7. Koolwijk P, Peters E, van der Vecht B, et al. Involvement of VEGFR-2 (kdr/flk-1) but not VEGFR-1 (flt-1) in VEGF-A and VEGF-C induced tube formation by human microvascular endothelial cells in fibrin matrices *in vitro*. Angiogenesis 2001;4:53–60.
8. Gerber H-P, McMurtrey A, Kowalski J, et al. Vascular endothelial growth factor regulates endothelial survival through the phosphatidylinositol 3′-kinase/Akt signal transduction pathway. Requirement for Flk-1/KDR activation. J Biol Chem 1998;273:30336–43.
9. Benjamin LE, Hemo I, Keshet E. A plasticity window for blood vessel remodelling is defined by pericyte coverage of the preformed endothelial network and is regulated by PDGF-B and VEGF. Development 1998;125:1591–8.
10. Bates DO, Heald RI, Curry FE, Williams B. Vascular endothelial growth factor increases Rana vascular permeability and compliance by different signalling pathways. J Physiol (Lond) 2001;533:263–72.
11. Rak J, Mitsuhashi L, Bayo L, et al. Mutant *ras* oncogenes upregulate VEGF/VPF expression: implications for induction and inhibition of tumour angiogenesis. Cancer Res 1995;55:4575–80.
12. Mukhopadhyay D, Knebelmann B, Cohen HT, Anath S, Sukhatme VP. The von Hippel-Lindau tumor suppressor gene product interacts with Sp1 to repress vascular endothelial growth factor promoter activity. Mol Cell Biol 1997;17:5629–39.
13. Zhou YZ, Xiong YX, Wu XT, et al. Inactivation of PTEN is associated with increased angiogenesis and VEGF overexpression in gastric cancer. World J Gastroenterol 2004;10:3225–9.
14. Shweiki D, Neeman M, Itin A, Keshet E. Induction of vascular endothelial growth factor expression by hypoxia and by glucose deficiency in multicell spheroids: implications for tumor angiogenesis. Proc Natl Acad Sci U S A 1995;92:768–72.
15. Tse V, Xu L, Yung YC, et al. The temporal-spatial expression of VEGF, angiopoietins-1 and -2, and Tie-2 during tumor angiogenesis and their functional correlation with tumor neovascular architecture. Neurol Res 2003;25:729–38.
16. Wiesmann C, Fuh G, Christinger HW, Eigenbrot C, Wells JA, de Vos AM. Crystal structure at 1.7 Å resolution of VEGF in complex with domain 2 of the Flt-1 receptor. Cell 1997;91:695–704.
17. Lu D, Kussie P, Pytowski B, et al. Identification of the residues in the extracellular region of KDR important for interaction with vascular endothelial growth factor and neutralizing KDR-antibodies. J Biol Chem 2000;275:14321–30.
18. Meyer M, Clauss M, Lepple-Wienhues A, et al. A novel vascular endothelial growth factor encoded by Orf virus, VEGF-E, mediates angiogenesis via signalling through VEGFR-2 (KDR) but not VEGFR-1 (Flt-1) receptor tyrosine kinase. EMBO J 1999;18:363–74.
19. Gille H, Kowalski J, Li B, et al. Analysis of biological effects and signalling properties of Flt-1 and KDR: a reassessment using novel highly receptor-specific VEGF mutants. J Biol Chem 2001;244:3222–30.
20. Takahashi T, Ueno H, Shibuya M. VEGF activates protein kinase-C dependent, but Ras-independent Raf-MEK-MAP kinase pathway for DNA synthesis in primary endothelial cells. Oncogene 1999;18:2221–30.
21. Rousseau S, Houle F, Kotanides H, et al. Vascular endothelial growth factor (VEGF)-driven actin-based motilityis mediated by VEGFR2 and requires concerted activation of stress-activated protein kinase 2 (SAPK2/p38) and geldanamycin-sensitive phosphorylation of focal adhesion kinase. J Biol Chem 2000;275:10661–72.
22. Carmeliet P, Lampugnani MG, Moons L, et al. Targeted deficiency or cytosolic truncation of the VE-cadherin gene in mice impairs VEGF-mediated endothelial survival and angiogenesis. Cell 1999;98:147–57.
23. Folkman J. Tumor angiogenesis: therapeutic implications. N Engl J Med 1971;285:1182–6.
24. Wood JM, Bold G, Buchdunger E, et al. PTK787/ZK 222584, a novel and potent inhibitor of vascular endothelial growth factor receptor tyrosine kinases, impairs vascular endothelial growth factor-induced responses and tumor growth after oral administration. Cancer Res 2000;60:2178–89.
25. Mendel DB, Laird AD, Xin X, et al. *In vivo* antitumor activity of SU11248, a novel tyrosine kinase inhibitor targeting vascular endothelial growth factor and platelet-derived growth factor receptors: determination of a pharmacokinetic/pharmacodynamic relationship. Clin Cancer Res 2003;9:327–37.
26. Beebe JS, Jani JP, Knauth E, et al. Pharmacological characterization of CP-547,632, a novel vascular endothelial growth factor receptor-2 tyrosine kinase inhibitor for cancer therapy. Cancer Res 2003;63:7301–9.
27. Sepp-Lorenzino L, Rands E, Mao X, et al. A novel orally bioavailable inhibitor of kinase insert domain-containing receptor induces antiangiogenic effects and prevents tumor growth *in vivo*. Cancer Res 2004;64:751–6.
28. Hennequin LF, Thomas AP, Johnstone C, et al. Design and structure-activity relationship of a new class of potent VEGF receptor tyrosine kinase inhibitors. J Med Chem 1999;42:5369–89.
29. Wedge SR, Ogilvie DJ, Dukes M, et al. ZD6474 inhibits vascular endothelial growth factor signaling, angiogenesis, and tumor growth following oral administration. Cancer Res 2002;62:4645–55.
30. Wedge SR, Ogilvie DJ, Dukes M, et al. ZD4190: an orally active inhibitor of vascular endothelial growth factor signaling with broad-spectrum antitumor efficacy. Cancer Res 2000;62:970–5.
31. Wild R, Ramakrishnan S, Sedgewick J, Griffioen AW. Quantitative assessment of angiogenesis and tumor vessel architecture by computer-assisted digital image analysis: effects of VEGF-toxin conjugate on tumor microvessel density. Microvasc Res 2000;59:368–76.
32. Zeng H, Sanyal S, Mukhopadhyay D. Tyrosine residues 951 and 1059 of vascular endothelial growth factor receptor-2 (KDR) are essential for vascular permeability factor/vascular endothelial growth factor-induced endothelium migration and proliferation, respectively. J Biol Chem 2001;276:32714–9.
33. Waltenberger J, Claesson-Welsh L, Siegbahn A, Shibuya M, Heldin CH. Different signal transduction properties of KDR and Flt-1, two receptors for vascular endothelial growth factor. J Biol Chem 1994;269:26988–95.
34. Rahimi N, Dayanir V, Lashkari K. Receptor chimeras indicate that the vascular endothelial growth factor receptor-1 (VEGFR-1) modulates mitogenic activity of VEGFR-2 in endothelial cells. J Biol Chem 2000;275:16986–92.
35. Hillman NJ, Whittles CE, Pocock TM, Williams B, Bates DO. Differential effects of vascular endothelial growth factor-C and placental growth factor-1 on the hydraulic conductivity of frog mesenteric capillaries. J Vasc Res 2001;38:176–86.
36. Hiratsuka S, Minowa O, Kuno J, Noda T, Shibuya M. Flt-1 lacking the tyrosine kinase domain is sufficient for normal development and angiogenesis in mice. Proc Natl Acad Sci U S A 1998;95:9349–54.
37. Autiero M, Waltenberger J, Communi D, et al. Role of PlGF in the intra- and intermolecular cross talk between the VEGF receptors Flt1 and Flk1. Nat Med 2003;9:936–43.
38. Karkkainen MJ, Haiko P, Sainio K, et al. Vascular endothelial growth factor C is required for sprouting of the first lymphatic vessels from embryonic veins. Nat Immunol 2004;5:74–80.
39. Onogawa S, Kitadai Y, Tanaka S, Kuwai T, Kimura S, Chayama K. Expression of VEGF-C and VEGF-D at the invasive edge correlates with lymph node metastasis and prognosis of patients with colorectal carcinoma. Cancer Sci 2004;95:32–9.
40. Arinaga M, Noguchi T, Takeno S, Chujo M, Miura T, Uchida Y. Clinical significance of vascular endothelial growth factor C and vascular endothelial growth factor receptor 3 in patients with nonsmall cell lung carcinoma. Cancer 2003;97:457–64.
41. Padera TP, Kadambi A, di Tomaso E, et al. Lymphatic metastasis in the absence of functional intratumor lymphatics. Science 2002;296:1883–6.
42. Shimizu K, Kubo H, Yamaguchi K, et al. Suppression of VEGFR-3 signaling inhibits lymph node metastasis in gastric cancer. Cancer Sci 2004;95:328–33.
43. Alam A, Herault J-P, Barron P, et al. Heterodimerization with vascular endothelial growth factor receptor-2 (VEGFR-2) is necessary for VEGFR-3 activity. Biochem Biophys Res Commun 2004;324:909–15.
44. Rubin BP, Singer S, Tsao C, et al. KIT activation is a ubiquitous feature of gastrointestinal stromal tumors. Cancer Res 2001;61:8118–21.
45. Beghini A, Ripamonti CB, Cairoli R, et al. KIT activating mutations: incidence in adult and pediatric acute myeloid leukaemia, and identification of an internal tandem duplication. Haematologica 2004;89:920–5.
46. Horner A, Bishop NJ, Bord S, et al. Immunolocalisation of vascular endothelial growth factor (VEGF) in human neonatal growth plate cartilage. J Anat 1999;194:519–24.
47. Petersen W, Tsokos M, Pufe T. Expression of VEGF121 and VEGF165 in hypertrophic chondrocytes of the human growth plate and epiphyseal cartilage. J Anat 2002;201:153–7.
48. Nakagawa M, Kaneda T, Arakawa T, et al. Vascular endothelial growth factor (VEGF) directly enhances osteoclastic bone resorption and survival of mature osteoclasts. FEBS Lett 2000;473:161–4.
49. Mayr-Wohlfart U, Waltenberger J, Hausser H, et al. Vascular endothelial growth factor stimulates chemotactic migration of primary human osteoblasts. Bone 2002;30:472–747.

Downloaded from http://aacrjournals.org/cancerres/article-pdf/65/10/4389/2531157/4389-4400.pdf by guest on 28 March 2025

**50.** Midy V, Plouet J. Vasculotropin/vascular endothelial growth factor induced differentiation in cultured osteoblasts. Biochem Biophys Res Commun 1994;199:380–6.

**51.** Zelzer E, Mamluk R, Ferrara N, Johnson RS, Schipani E, Olsen BR. VEGFA is necessary for chondrocyte survival during bone development. Development 2004; 131:2161–71.

**52.** Gerber H-P, Vu TH, Ryan AM, Kowalski J, Werb Z, Ferrara N. VEGF couples hypertrophic cartilage remodeling, ossification and angiogenesis during endochondral bone formation. Nature Med 1999;5:623–8.

**53.** Haigh JJ, Gerber H-P, Ferrara N, Wagner EF. Conditional inactivation of VEGF-A in areas of collagen2a1 expression results in embryonic lethality in the heterozygous state. Development 2000;127:1445–53.

**54.** Modlich U, Kaup FJ, Augustin HG. Cyclic angiogenesis and blood vessel regression in the ovary: blood vessel regression during luteolysis involves endothelial cell detachment and vessel occlusion. Lab Invest 1996; 74:771–80.

**55.** Ferrara N, Chen H, Davis-Smyth T, et al. Vascular endothelial growth factor is essential for corpus luteum angiogenesis. Nat Med 1998;4:336–40.

**56.** Zimmermann RC, Xiao E, Bohlen P, Ferin M. Administration of antivascular endothelial growth factor receptor-2 antibody in the early follicular phase delays follicular selection and development in the rhesus monkey. Endocrinology 2002;143:2496–502.

**57.** Ryan AM, Eppler DB, Hagler KE, et al. Preclinical safety evaluation of rhuMAbVEGF, an antiangiogenic humanized monoclonal antibody. Toxicol Pathol 1999; 27:78–86.

**58.** Inai T, Mancuso M, Hashizume H, et al. Inhibition of vascular endothelial growth factor (VEGF) signaling in cancer causes loss of endothelial fenestrations, regression of tumor vessels, and appearance of basement membrane ghosts. Am J Pathol 2004;165:35–52.

**59.** Kiessling F, Farhan N, Lichy MP, et al. Dynamic contrast-enhanced magnetic resonance imaging rapidly indicates vessel regression in human squamous cell carcinomas grown in nude mice caused by VEGF receptor 2 blockade with DC101. Neoplasia 2004;6:213–23.

**60.** Yuan F, Chen Y, Dellian M, Safabakhsh N, Ferrara N, Jain RK. Time-dependent vascular regression and permeability changes in established human tumor xenografts induced by an anti-vascular endothelial growth factor/vascular permeability factor antibody. Proc Natl Acad Sci U S A 1996;93:14765–70.

**61.** Hurwitz H, Fehrenbacher L, Novotny W, et al. Bevacizumab plus irinotecan, fluorouracil, and leucovorin for metastatic colorectal cancer. N Engl J Med 2004;350:2335–42.

**62.** Willett CG, Boucher Y, di Tomaso E, et al. Direct evidence that the VEGF-specific antibody bevacizumab has antivascular effects in human rectal cancer. Nat Med 2004;10:145–7.

**63.** Joukov V, Sorsa T, Kumar V, et al. Proteolytic processing regulates receptor specificity and activity on VEGF-C. EMBO J 1997;16:3898–911.

**64.** Jia H, Bagherzadeh A, Bicknell R, Duchen MR, Liu D, Zachary I. Vascular endothelial growth factor (VEGF)-D and VEGF-A differentially regulate KDR-mediated signaling and biological function in vascular endothelial cells. J Biol Chem 2004;279:36148–57.

**65.** Koolwijk P, Peters E, van der Vecht B, et al. Involvement of VEGFR-2 (kdr/flk-1) but not VEGFR-1 (flt-1) in VEGF-A and VEGF-C induced tube formation by human microvascular endothelial cells in fibrin matrices *in vitro*. Angiogenesis 2001;4:53–60.

**66.** Jayson GC, Zweit J, Jackson A, et al. Molecular imaging and biological evaluation of HuMV833 anti-VEGF antibody: implications for trial design of antiangiogenic antibodies. J Natl Cancer Inst 2002;94:1484–93.

**67.** Medinger M, Mross K, Zirrgiebel U, et al. Phase I dose escalation study of the highly potent VEGF receptor tyrosine kinase inhibitor, AZD2171, in patients with advanced cancers with liver metastases. Proc Am Soc Clin Oncol 2004;23:208.


Downloaded from http://aacrjournals.org/cancerres/article-pdf/65/10/4389/2531157/4389-4400.pdf by guest on 28 March 2025